J. exp. Biol. ***190****, 195–215 (1994)*
Printed in Great Britain © The Company of Biologists Limited 1994

SCALE EFFECTS ON THE STRESSES AND SAFETY FACTORS IN THE WING BONES OF BIRDS AND BATS

SEAN J. KIRKPATRICK*,†

Department of Biology, University of Miami, Coral Gables, FL 33124, USA

Accepted 22 November 1993

Summary

The effects of scale on the estimated stresses and safety factors in the humeri of several bird and bat species were investigated. This was accomplished by estimating the lift distribution across the wings at two extremes of flight, gliding flight and the downstroke in hovering, finding the center of lift on the wings at these two extremes and calculating the applied bending and twisting moments. This information, along with measurements of mechanically important morphological variables, allowed for estimates of bending and shearing stresses in the humeri for both gliding flight and on the downstroke in hovering. The stresses in flapping flight other than hovering should fall somewhere between these two values. It was found that the stresses in the humeri are not scale-dependent and that the bending stresses are slightly lower than those found in the limbs of terrestrial animals, while the shearing stresses are larger than those in terrestrial limbs. The breaking stress of bird and bat wing bone was also investigated. Both materials were found to have a lower breaking stress than that of typical long bone material. The ratio between the breaking stress of the material and the estimated stresses was defined as the safety factor. Bird humeri have safety factors that are generally greater than those of bat humeri. This is because bat bone has a lower breaking stress than does bird bone, although the estimated stresses in the wings are similar. The mean safety factor against failure due to bending in gliding flight was 6.63 for birds and 3.99 for bats. In hovering, the mean safety factors against failure due to bending were 2.22 for birds and 1.41 for bats. The safety factors against failure due to shearing stresses were estimated to be seven time greater than those against failure due to pure bending stresses.

Introduction

The main function of wing bones is to transmit a force to the external environment during flight. In the act of imparting these forces, the bones inevitably deflect to some degree, but they must not deflect too far or the wings will cease to function as effective aerofoils. Likewise, they must be strong enough not to fail under the imposed loads. This means that the bones need to be stiff and strong.

*Present address: The Johns Hopkins University, School of Medicine, Baltimore, MD 21205, USA.
†Mailing address: The Johns Hopkins University, Applied Physics Laboratory, Johns Hopkins Road, Laurel, MD 20723-6099, USA.

Key words: bird, bat, wing, stress, safety factor, scaling.

While the geometry of a structure determines the stress levels and distributions in a structure under a load, the breaking stress of the structural material provides an upper limit on the stresses that a structure can achieve without catastrophic failure. Therefore, any investigation into the stresses in the wing bones during flight must consider both the morphology of the wings and bones and the mechanical properties of the wing bone material. The goals of this study therefore were (1) to investigate the scaling relationships between body size and several morphological variables of bird and bat wings that must be known in order to estimate the stress levels in the wings, (2) to measure the breaking stress of bird and bat wing bone material, and (3) to estimate the bending and shearing stresses in the wing bones during two extreme modes of flight, gliding and the downstroke of hovering, and determine whether these stresses are in any way scale-related. Safety factors against failure were also calculated for the two flight regimes.

Materials and methods

General

The selection of organisms for this study was somewhat arbitrary and, for the birds, highly opportunistic. The main goal of the study was to obtain a wide variety of species representing as many different body masses, wing shapes and ecologies as possible. Most of the birds were obtained from avian rehabilitation centers, where they had died and been immediately frozen, or were found along roadsides or beneath windows. Upon collection, body masses and external morphological measurements were taken as soon as possible and the animals were frozen until needed further. Most of the bats were collected in Costa Rica during August 1989, although some of the measurements of body mass, wing span and wing area come from bats mist-netted in Bahia Kino, Sonora, Mexico, or in various locations in Peru (C. Sahley, personal communication). In all cases, body mass, wing spans and wing areas were taken as soon as possible after collection and the bats were frozen until required for further aspects of the study. Because of the large size range of animals used in this study, it was assumed that the intraspecific variation was small compared with the interspecific variation and, therefore, each individual was considered to be representative of its species.

The main portion of this study included 14 species of birds and 9 species of bats, although body masses, wing spans, wing areas and wing moments of inertia about the shoulder joint were taken for other species and are included in the analysis of these variables. All of the measurements are for adult individuals. Few data on wing morphology were taken from the literature, as the methods used to obtain the information are widely variable and, in most cases, it is not very clear how the measurements were taken.

In order to investigate the scaling patterns of the morphological variables, allometric plots of the morphological data were constructed, lines of best fit of the form $y=ax^m$ were drawn through the data points using the reduced major axis method (r.m.a.) (Rayner, 1985; Hofman, 1988) and 95 % fiducial limits about the line were calculated. The slopes, m, of the lines indicate how the variables scale in relation to each other. t-tests were conducted to examine the differences in either the scaling patterns or the magnitudes of

the measured variables between birds and bats and also to test against the predictions of geometric similarity.

Body mass, wing span and wing area

To obtain wing measurements of birds, the methods of Pennycuick (1989) were followed and for bats, the methods of Norberg (1990) were used. Wing span, b, is defined as the greatest tip-to-tip measurement of the fully extended wings. Wing area, S, is the total projected area of both wings including the portion of the body between the wing roots.

Second moment of area of the wing about the shoulder joint

Weis-Fogh (1973) showed, in a quasi-steady analysis of hovering animals, that the mean lift force should be proportional to the second moment of area of the wing about the wing base. The second moment of area of the wings about the wing base, Q_2, was approximated here as:

$$Q_2 = \Sigma(a^2 S_a)\,, \tag{1}$$

where S_a is the area of an elemental strip of wing a distant from the shoulder joint. These values were determined by photographing the wings, along with a scale, with a 100 mm f2.8 macro lens, dividing the print of the wing into 10 chord-wise strips and summing the sectional second moments of area across the entire wing.

Wing moment of inertia about the shoulder joint

The moment of inertia of a wing, I_w, depends upon the distribution of mass along the wing. Its value must be known in order to calculate the internal torque imposed upon the wing during flapping flight (Ellington, 1984), and it is also one of the variables that affects flapping frequency (Pennycuick, 1990). The moment of inertia of the wings about the shoulder joints was approximated as:

$$I_w = \Sigma(m_r r^2)\,, \tag{2}$$

where m_r is the mass of an elemental strip r distant from the shoulder joint. In practice, the moment of inertia of the wings was found by dividing the wings into 10 chord-wise strips of equal width and assuming that the span-wise center of mass of each strip was located at the span-wise center of each strip. The distance from the shoulder joint to the center of each strip was measured and the strips were weighed. Equation 2 was then employed to estimate I_w. This method has been used previously for insects (Sotavalta, 1954; Ellington, 1984), birds (Kirkpatrick, 1990) and Old World bats (Thollesson and Norberg, 1991).

Second and polar moments of area of bone cross sections

The second moment of area, I, and the polar moment of area, J, of a cross section of a beam are measures of how much material is present and of how this material is distributed about a given axis and the centroid, respectively. The values are of importance when considered in the context of a bending and twisting beam. Wainwright *et al.* (1976) give a complete derivation of these variables, as does any text on elementary mechanics, and

therefore a derivation will not be given here. The second moments of area of irregular cross sections (such as those of wing bones) about the major bending axis may be approximated as:

$$I = \Sigma(y^2 S_i)\,, \tag{3}$$

where S_i is the area of an elemental strip y distant from the neutral axis. The term $\Sigma(yS_i)$, where y is now the vertical distance from some arbitrary axis, is an approximation to the first moment of area of the section and represents an analytical method of locating the centroid and neutral axes of the section. Likewise, the polar moments of area, J, of thin-walled irregular cross sections may be approximated as:

$$J = \Sigma(r^2 S_j)\,, \tag{4}$$

where S_j is the area of a ring of material at a radius r from the centroid of the section. It should be noted here that, assuming geometric similarity, from the above equations both I and J should vary as the fourth power of length, so a small increase in radius will result in a large increase in I and J.

Cross sections of the wing bones were made at the proximal ends of the humerus, just distal to the insertion of the flight muscles, at the proximal and distal ends of the radio-ulna (radius in bats) and at the proximal end of the metacarpus. From these sections, the second and polar moments of area, the maximum outside radius, r, and the maximum vertical distance from the neutral axis to the outside wall, y, were measured. In the case of the radio-ulnae, the bones were positioned relative to each other as they would be in gliding flight. The cross sections were photographed, along with a scale, with a 100 mm f2.8 macro lens. In the case of some of the smaller bones, a doubler was used to provide additional magnification. The prints were projected onto an Amiga 1000 computer screen *via* a video interface, and the inside and outside perimeters of the cross sections were traced along with a portion of a scale using a drawing program (Aegis Draw Plus, Aegis Development). A BASIC program located the neutral axes (above), and thus the centroid of each section, and then calculated the second and polar moments, as well as r and y. Using this method to calculate these variables on objects of known second and polar moments of area revealed that this method resulted in a maximum error of 3 %.

Breaking stress of bird and bat wing bone

Typical hourglass-shaped tensile test pieces were machined from the dorsal surfaces of the humeri of great blue herons (*Ardea herodias*), great white herons (*Ardea occidentalis*) and brown pelicans (*Pelecanus occidentalis*) and from the humeri of the bats *Desmodus rotundus* and *Artibeus jamaicensis*. These species were selected primarily on the basis of their large size. All of the animals were frozen in air-tight bags immediately upon death; there is no reason to suspect any *post-mortem* deterioration of the bone material. Test pieces were cut along the long axis of the humeri while under continuous irrigation to prevent the bones from drying or appreciably warming. A typical test piece for the bird bone was 1 cm long and 1 mm^2 in cross-sectional area. Bat samples were somewhat smaller.

An Instron model 1000 universal testing instrument fitted with a 50 kg weigh beam was

used in all of the experiments. The test pieces were monotonically loaded to failure at room temperature over a series of strain rates ranging from $\dot{\epsilon}$=0.017 s^{-1} to $\dot{\epsilon}$=0.333 s^{-1}. The output from the weigh beam was fed to an Omniscribe series D5000 chart recorder to produce force–time graphs from which the breaking stress, σ_{ult}, was calculated. The samples were kept moist throughout the duration of the tests. Owing to the small sizes and slipperiness of the test pieces, gripping was a problem. After much trial and error, it was found that modified four-pronged collet-type clamps provided a secure grip while not inducing any noticeable local stress concentrations. If slippage at the grips was observed (by marks placed on the test pieces) or if the sample broke in the vicinity of the grips, the test was eliminated from the data set.

Moments, stresses and safety factors: predictions of geometric similarity

The proximal end of a flying animal's humerus, just distal to the insertions of the flight muscles, must be strong enough to withstand the bending and twisting moments transmitted to it by the lifting forces acting on the wing during gliding flight. Assuming that the body generates no lift, and because the proximal end of the humerus has a full 6° of freedom of movement and therefore cannot transmit these moments to the body without the aid of flight muscles, then each wing must support half of the weight of the bird or bat. Similarly, each wing bone must resist the moments imparted to it by the portion of the wing distal to it. Drag also imposes moments on the wings, but the drag-induced moments are probably much smaller than the weight-induced moments and therefore are ignored here.

The bending and twisting moments on the wings, being the product of half of the weight of the animal per wing and a moment arm, should scale as the fourth power of length, assuming geometric similarity. Here, the moment arm is the distance from the center of lift of the wing to the axis of bending or torsion. Since the maximum bending stress, σ_b, in a beam in simple bending is given by:

$$\sigma_b = M_b y/I\,, \tag{5}$$

where M_b is the bending moment and y and I are as above, the bending stress in a wing bone should increase directly with length, if the wings scale geometrically. A similar line of reasoning can be followed for shearing stress. The shear stress, τ, in a beam is given by:

$$\tau = Tr/J\,, \tag{6}$$

where T is the torque and r and J are as above.

So, if we assume geometric similarity, then both the bending and shearing stresses should increase directly with wing span.

The procedure for calculating the moments and stresses essentially follows that of Pennycuick (1967). The moments were estimated at three points along the wings; the proximal end of the humerus, just distal to the insertion of the flight muscles, and the proximal and distal ends of the radio-ulna (radius). In order to do this, an estimate of the lift distribution across the wings had to be made. This was attempted for two extreme flight conditions, gliding flight and the downstroke of hovering.

To estimate the lift distributions, each wing was divided into 10 chord-wise strips

and the lift on each strip was assumed to be proportional to its planform area multiplied by the square of the local relative airspeed. That is, it was assumed that there was a constant sectional lift coefficient along the wing. The lift on each section was then assumed to act at the span-wise center of each strip and a quarter-chord back from the leading edge. This follows from the theory of thin wing sections (Abbott and Von Doenhoff, 1959). In gliding flight, the local relative airspeed is assumed to be constant across the wing span. In hovering, however, the local relative airspeed is zero at the shoulder and increases linearly along the wing to a maximum of $r\omega$ at the wing tip, where r is the distance from the shoulder to the wing tip and ω is the angular velocity in rad s^{-1}. In flapping flight other than hovering, the local relative airspeed is between these two extremes.

The axes of bending and twisting were arranged perpendicular to one another, with the twisting axis running parallel to and along the long axis of the bones. The bending axes were then perpendicular to the long axes of the bones at the locations listed above. To estimate the applied moments at any point along the wing, two things must be known: (1) what portion of the animal's weight is supported at that point of the wing and (2) over what distance this force acts, the moment arm. The method of determining these moment arms differs between gliding and hovering flight.

In gliding flight, since the local relative air velocity and the local lift coefficient are assumed to be constant across the span, the lift force on each elemental strip of wing is directly proportional to its planform area. Thus, by multiplying the planform area of each strip, S_i, by its distance to the bending or twisting axis, r_i, and summing these values across the entire portion of the wing that is distal to the bending axis, we can arrive at a value for the first moment of area, Q_1, of the wing about the bending or twisting axis;

$$Q_{1b} = \Sigma(r_{bi}S_i)\,, \tag{7}$$

for bending and

$$Q_{1t} = \Sigma(r_{ti}S_i)\,, \tag{8}$$

for twisting,where r_i is the moment arm of strip i (r_b for bending and r_t for twisting) and S_i is the projected area of strip i. By dividing the first moment of area by the total area of the wing distal to the bending axis, values of mean bending, $\overline{r_{bg}}$, and twisting, $\overline{r_{tg}}$, arms can be found for any point along the wing for gliding flight.

Since the lift on each strip was assumed to be proportional to its area, whatever fraction of the wing that is distal to the bending axis supports the same fraction of half of the weight. Thus, we have all the information that is needed to estimate the bending and twisting moments imparted to any point of the wing in gliding flight. The bending, M_{bg}, and twisting, T_b, moments imparted to any point along the wing in gliding flight are then defined as:

$$M_{bg} = K(\tfrac{1}{2}m\boldsymbol{g})\overline{r_{bg}} \tag{9}$$

and

$$T_g = K(\tfrac{1}{2}m\boldsymbol{g})\overline{r_{tg}}\,, \tag{10}$$

where K is a constant that depends upon what portion of the weight of the animal is supported by the area of the wing distal to the bending axis and $\boldsymbol{g}$ is the acceleration due to

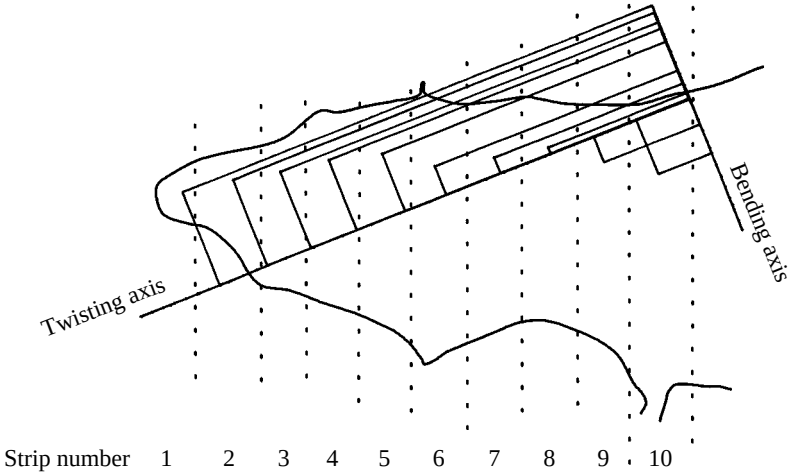

Fig. 1. Moment diagram for the proximal end of the humerus of a bat's wing. See text for further explanation.

gravity. K=1 if the bending axis is about the proximal head of the humerus and K=0 at the wing tip. Fig. 1 is a moment diagram for the humerus of a bat wing. The bending and twisting axes are perpendicular to one another, with the twisting axis running along the long axis of the bones.

As discussed earlier (equation 1), the second moment of area, Q_2, of a wing about its base can be approximated as:

$$Q_2 = \Sigma(a^2 S_a)\,,$$

where S_a is the area of a strip of wing a distant from the shoulder joint (Weis-Fogh, 1973). Thus, by taking the sectional second moment of area of each strip, multiplying it by its respective bending or twisting arm, summing across the wing portion distal to the bending axis, and then dividing by the total second moment of area of the wing portion distal to the bending axis, we can arrive at values for the mean bending arm, $\overline{r_{bh}}$, and mean twisting arm, $\overline{r_{th}}$, for the downstroke in hovering:

$$\overline{r} = \frac{\Sigma(a^2 S_a)_i r_i}{\Sigma(a^2 S_a)_i}\,. \tag{11}$$

The same method can be used here to estimate what fraction of the animal's weight is supported by the portion of the wing that is distal to the bending axis, as was done for the gliding case. However, in hovering, lift is not produced over the entire wing-stroke cycle, but only during some portion of it. If we make the rough assumption that lift is generated only during half of the cycle (the downstroke), then the bending, M_{bh}, and twisting, T_h, moments in the downstroke of hovering are defined as:

$$M_{bh} = 2K(\tfrac{1}{2}m\boldsymbol{g})\overline{r_{bh}} \tag{12}$$

and

$$T_h = 2K(\tfrac{1}{2}m\boldsymbol{g})\overline{r_{th}}\,. \tag{13}$$

Bending stresses, shearing stresses and safety factors in the humeri

Equations 5 and 6 were used to estimate the bending and shearing stresses imposed upon the proximal ends of the humeri in both gliding flight and in the downstroke of hovering flight. Bending and twisting moments were taken from equations 9–13. The values of I, J, y and r were taken from the computer images of the cross sections of the humeri generated above.

Safety factors, that is the ratio between the breaking stress of bird or bat wing bone and the estimated stresses, were calculated for both loading situations. A value of 75 % of the breaking stress of wing bone in tension was used as the breaking stress of wing bone in shear. This assumption is based on Yamada (1970), who reported on the mechanical properties of compact bone taken from the long bones of cattle, horses and pigs. He showed that the ultimate shear strengths of bovine, equine and porcine compact bone loaded in torsion were, respectively, 76, 81 and 67 % of the same material loaded in tension.

Results and Discussion

Morphological variables

Table 1 lists the species and external morphological measurements for the animals used in the main portion of this study. Table 2 gives the reduced major axis (r.m.a.) slopes and the 95 % fiducial limits about the lines when the morphological variables were plotted against wing span. The allometric equations for all of the morphological relationships examined here are given in the Appendix. As Table 2 shows, very few variables scale in a manner other than that predicted by geometric similarity when plotted as a function of wing span. The only exceptions being the already well established (e.g. Greenwalt, 1962, 1975) relationships between body mass, wing span and wing area in birds.

No significant correlation was found between the polar moment of area of the metacarpus of bats and wing span. All of the other correlation coefficients, for both birds and bats, were highly significant ($P<0.05$).

The only significant difference seen between the scaling patterns of bird and bat wings was previously reported by Tholleson and Norberg (1991). They published an account of the effects of scale on the wing moment of inertia of Old World bats and found that, unlike birds (Kirkpatrick, 1990), the wing moment of inertia of Old World bats scales nearly geometrically in relation to body mass. The equations estimated here for neotropical bats (equation A4b in the Appendix) do not differ significantly in either slope or y-intercept from those obtained by Tholleson and Norberg, so combining their data with the data collected here we get:

$$I_w = 2.05 \times 10^{-3} m_b^{1.61} \quad (14)$$

when bat wing moment of inertia is plotted as a function of body mass (95 % fiducial limits 1.78, 1.45; r=0.982) and:

$$I_w = 8.52 \times 10^{-4} b^{4.96} \quad (15)$$

when plotted against wing span (95 % fiducial limits 5.22, 4.72; r=0.982) for bats in

Table 1. *External morphological measurements of the animals used in this study*

Species	m_b (kg)	b (m)	S (m^2)	Q_2 ($\times10^{-3}\,m^4$)	I_w ($\times10^{-3}\,kg\,m^2$)
Birds					
Falco sparverius	0.072	0.59	0.042	0.432	0.587
Mimus polyglottos	0.041	0.36	0.027	0.0797	*
Vireo olivaceous	0.019	0.24	0.0103	0.0107	*
Seiurus aurocapillus	0.020	0.24	0.011	0.0112	*
Bubulcus ibis	0.250	0.882	0.114	1.43	0.465
Phalacrocorax auritus	1.5	1.31	0.2095	9.03	3.03
Rallus longirostrus	0.220	0.525	0.054	0.247	*
Larus atricilla	0.305	1.09	0.0114	3.67	*
Otus asio	0.094	0.54	0.0475	0.227	*
Catoptrophorus semipalmatus	0.210	0.70	0.0632	0.654	*
Buteo platypterus	0.295	0.93	0.015	2.85	*
Puffinus lherminieri	0.082	0.625	0.046	0.43	*
Gavia immer	2.5	1.30	0.156	*	*
Ardea occidentalis	2.36	1.91	0.483	*	*
Bats					
Artibeus phaeotis	0.011	0.285	0.0129	0.0180	0.00174
Rhogeessa tumida	0.004	0.216	0.0077	0.0084	0.000382
Artibeus jamaicensis	0.0365	0.418	0.0252	0.0867	0.0177
Glossophaga soricina	0.010	0.271	0.0115	0.0155	0.00158
Tonatia sp.	0.012	0.265	0.141	0.0133	0.00131
Carillia perspicillata	0.0195	0.35	0.0194	0.0446	0.00357
Sturnira lilium	0.018	0.300	0.0145	0.0224	0.00261
Desmodus rotundus	0.031	0.398	0.0250	0.0656	0.00930
Phyllostomus discolor	0.039	0.465	0.0312	0.115	0.0195

m_b, body mass; b, wing span; S, wing area; Q_2, second moment of area about the shoulder joint; I_w, moment of inertia about the shoulder joint.

An asterisk indicates that a value was not obtained.

Other values of bird I_w are in Kirkpatrick (1990).

general. The slope of equation 14 differs significantly from that of birds, which is 2.05 (Kirkpatrick, 1990). This is due to the allometric relationship between body mass and wing span in birds. Neither the slope nor the *y*-intercept of equation 15 differs significantly from that found in birds.

For further comparison, the wing moments of inertia were also calculated for 15 insects, including lepidopterans, coleopterans, odonates and a dipteran. The body masses ranged from 8.04×10^{-6} to 4.5×10^{-3} kg and the wing spans from 0.021 to 0.155 m. The equations relating wing moment of inertia to body mass and wing span in insects are, respectively:

$$I_w = 8.05 \times 10^{-3} m_b^{2.003} \quad (16)$$

(95 % fiducial limits 2.84, 1.42; r=0.786) and:

$$I_w = 3.06 \times 10^{-4} b^{4.74} \quad (17)$$

Table 2. *Reduced major axis slopes (and 95 % fiducial limits) of the morphological variables as a function of wing span*

Variable	Units	Geometric similarity	Birds	Bats
m_b	kg	3.0	2.44 (2.65, 2.24)*	3.22 (3.74, 2.77)
S	m^2	2.0	1.78 (1.89, 1.67)*	1.83 (2.21, 1.51)
Q_2	m^4	4.0	3.87 (4.10, 3.65)	3.66 (4.00, 3.35)
I_w	$kg\,m^2$	5.0	5.08 (5.38, 4.80)†	4.96 (5.22, 4.72)
I_h	m^4	4.0	4.19 (4.45, 3.94)	4.42 (4.97, 3.92)
I_{pru}	m^4	4.0	4.22 (4.55, 3.91)	3.87 (4.80, 3.13)
I_{dru}	m^4	4.0	3.46 (4.38, 2.74)	4.53 (6.62, 3.08)
I_m	m^4	4.0	3.62 (4.86, 2.69)	3.17 (5.80, 1.73)
J_h	m^4	4.0	4.23 (4.52, 3.95)	4.38 (4.94, 3.88)
J_{pru}	m^4	4.0	3.88 (4.14, 3.63)	3.79 (4.45, 3.23)
J_{dru}	m^4	4.0	3.63 (4.64, 2.84)	4.36 (6.13, 3.11)
J_m	m^4	4.0	3.86 (5.78, 2.58)	No significant relationship

m_b, body mass; S, wing area; I_w, wing moment of inertia about the shoulder joint; $I_{h,pru,dru,m}$, second moment of area of the humerus, proximal radio-ulna (radius in bats), distal radio-ulna (radius) and metacarpus, respectively; $J_{h,pru,dru,m}$, polar moment of area of the humerus, proximal radio-ulna (radius), distal radio-ulna (radius) and metacarpus, respectively.

* indicates a departure from geometric similarity.

†From Kirkpatrick (1990).

(95 % fiducial limits 5.16, 4.35; r=0.0989). Neither line differs significantly in slope from the predictions of geometric similarity.

It is interesting to note that, although there were no statistical differences found between the absolute magnitudes of the morphological variables in birds and bats, the bat reduced major axis lines were nearly always slightly below the bird reduced major axis lines (Fig. 2). This was especially noticeable at the lower end of the scale size examined. This may be due in part to the small number of very small birds and large bats examined, as well as to decreasing video resolution at small sizes. In order to clarify this, more data are needed on small birds such as warblers (e.g. family Parulidae) and large bats such as *Vampyrum, Chrotopterus, Noctilio* and members of the Megachiroptera.

Breaking stress of bird and bat wing bone

Table 3 lists the mean values and standard deviations of the breaking stress of bird and bat wing bone. No differences were observed within the bird species nor within the bat species (t-tests, P>0.05), so the results are given under the general headings ‘bird humerus bone’ and ‘bat humerus bone’.

The breaking strength of bird humerus bone was found to be towards the lower end of the spectrum of reported breaking strengths of bone. It was approximately 125 MPa at all strain rates. The breaking stress of bat humerus bone (mean of 75 MPa) was significantly lower than that found in bird humerus bone and much lower than that reported in the

literature for other mammalian long bone. In an extensive list of the mechanical properties of amniote bone (Currey, 1987), only bone from the tympanic bulla of the fin whale had a lower breaking stress.

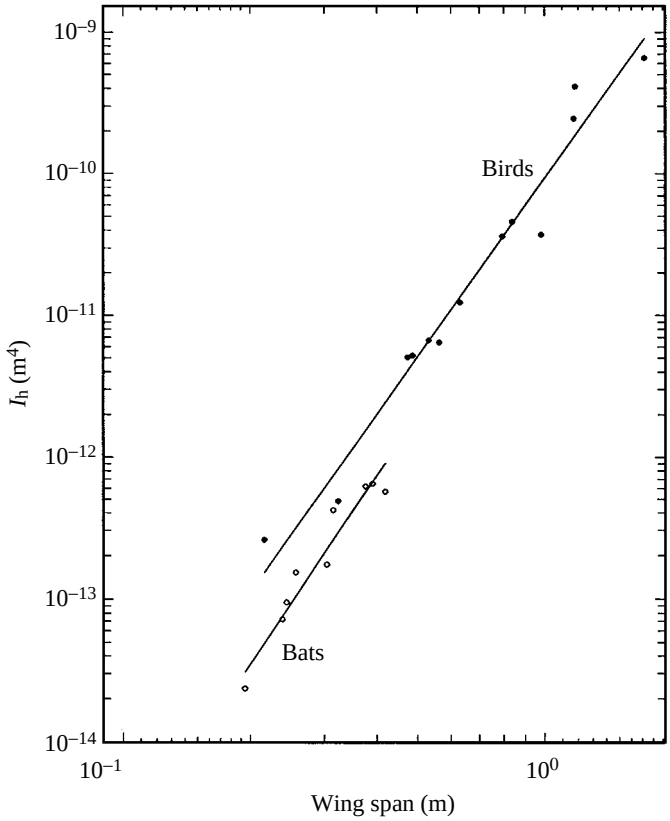

Fig. 2. Second moment of area of the proximal end of the humerus *versus* wing span for birds (filled circles) and bats (open circles). The slope of the bird line is 4.19 and that of the bat line is 4.42. Neither slope differs from that predicted by geometric similarity.

Table 3. *Breaking stress of bird and bat wing bone material*

	$\dot{\epsilon}$ (s^{-1})	σ_{ult} (MPa)	N
Bird humerus bone	0.023	130 (28)	6
	0.033	120 (0.8)	7
	0.083	120 (13)	5
	0.333	130 (66)	6
Bat humerus bone	0.017	78 (16)	6
	0.071	71 (35)	4

$\dot{\epsilon}$, strain rate; σ_{ult}, breaking stress.
Values in parentheses are standard deviations.

Table 4. *Reduced major axis slopes and 95 % fiducial limits of the bending and twisting moments at three points along the wing when plotted as a function of wing span*

Moment	Humerus	Proximal radio-ulna (radius)	Distal radio-ulna (radius)
Bird gliding			
Bending	3.24 (3.82, 2.75)†	3.19 (3.71, 2.74)†	3.21 (4.43, 2.33)
Twisting	3.60 (4.43, 2.89)	3.08 (3.70, 2.56)†	3.02 (4.80, 1.90)
Bird hovering			
Bending	3.26 (3.84, 2.77)†	3.23 (3.74, 2.78)†	3.20 (4.31, 2.37)
Twisting	3.49 (4.30, 2.84)	3.13 (3.71, 2.63)†	3.00 (4.70, 1.91)
Bat gliding			
Bending	3.87 (4.48, 3.35)	4.19 (4.99, 3.51)*	4.49 (5.74, 3.52)*
Twisting	5.75 (8.69, 3.80)*	3.96 (5.16, 3.04)	3.88 (5.66, 2.66)
Bat hovering			
Bending	3.20 (3.70, 2.77)†	4.19 (5.07, 3.45)*	4.57 (5.76, 3.62)*
Twisting	4.72 (6.60, 3.37)	3.80 (5.22, 2.76)	3.94 (5.68, 2.73)

The slope predicted by geometric similarity for all of the cases was 4.0.
† indicates a departure from geometric similarity.
* indicates a significant difference ($P<0.05$) between the bird and bat slopes.

Bending and twisting moments

Table 4 gives the slopes of the r.m.a. lines and the 95 % fiducial limits about the slopes generated by plotting the bending and twisting moments in gliding flight and in the downstroke of hovering against wing span. The slope predicted by geometric similarity is 4.0 and in 7 of the 24 cases (those that do not include 4.0 within their fiducial limits) the slopes estimated from the data differ from that predicted at a probability level of 0.05. Those that do not scale geometrically all increase more slowly than predicted. The slopes of the lines varied between birds and bats in nearly half the cases, notably the bending moments on the radio-ulna (radius) in gliding and in the downstroke in hovering. In every case where birds and bats differed, the slope was steeper for bats. Every correlation coefficient was highly significant ($P<0.01$). Fig. 3 is a plot of the bending moment about the proximal end of the humerus *versus* wing span in gliding for both birds and bats. Fig. 4 is a plot of the twisting moments at the same location, also in gliding flight.

Bending and shearing stresses in the humeri

As equations 5 and 6 indicate, values of the maximum vertical distance from the neutral axis, y, and maximum outside radius, r, are needed to calculate the maximum stress in the bones in bending and shearing, respectively. It is therefore of interest to examine the scaling patterns of these variables. When y is plotted against wing span for sections taken at the proximal end of the humeri just distal to the insertion of the flight muscles for both birds and bats, neither the slopes nor the y-intercepts of the two lines differ significantly from each other ($P>0.05$), and neither slope, 1.07 (95 % fiducial limits of 1.29 and 0.887) for the birds and 1.11 (95 % fiducial limits of 1.87 and 0.655) for the

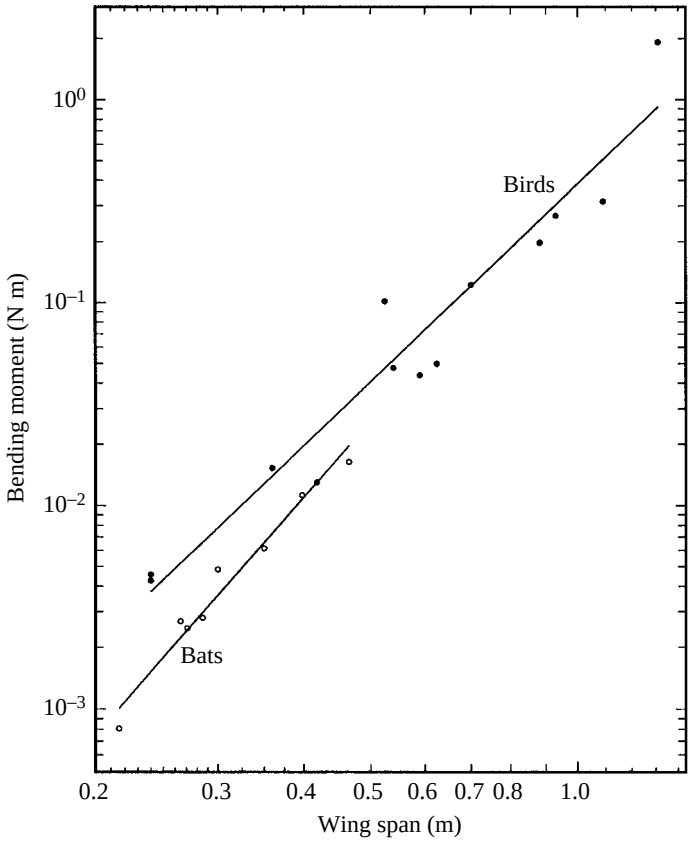

Fig. 3. Bending moments applied to the proximal end of the humeri in gliding flight as a function of wing span. The slope of the bird reduced major axis line (filled circles) is 3.24. That of the bat line (open circles) is 3.87. The slope of the bird line differs from that predicted by geometric similarity.

bats, differs from that predicted by geometric similarity (slope of 1.0). Likewise, neither the slopes (1.29 and 1.16, for birds and bats, respectively) nor the *y*-intercepts differ significantly from each other or from the predictions of geometric similarity (slope of 1.0) when maximum outside radius is plotted against wing span.

No significant relationship was found between either the bending or shearing stresses and wing span during gliding flight or on the downstroke in hovering and in no case was the mean stress value different between birds and bats ($P>0.05$). Fig. 5A,B plots bending stress as a function of wing span in gliding flight and in the downstroke of hovering, respectively. The correlation coefficients (0.197 and 0.161) of the r.m.a. lines drawn through the data are not significantly different from zero ($P\gg0.05$), indicating that bending stress is not scale-dependent. The plots of shearing stress *versus* wing span are similar, except that the magnitudes of these stresses are approximately one-seventh of those of bending. Again, the correlation coefficients are not significantly different from zero ($P\gg0.05$), indicating that shear stress is also not dependent on scale. Table 5 lists the values of the bending and shearing stresses for 11 birds and 7 bats. All of the estimated

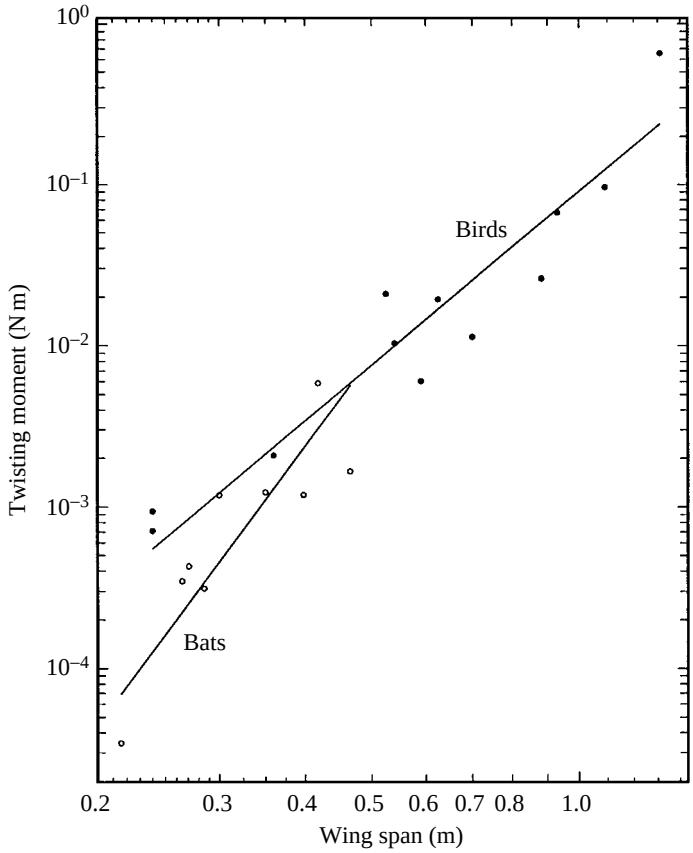

Fig. 4. As Fig. 3, but with twisting moments. The slope of the bird line (filled circles) is 3.60 and that of the bat line (open circles) is 5.75. Neither slope differs from the predictions of geometric similarity.

bending stresses except for one (that of the bat *Phyllostomus discolor* on the downstroke in hovering) are well below the tensile breaking stress of bird and bat wing bone material, and even when the maximum shearing strength of wing bone is set as 75 % of its tensile strength, the shearing stresses are also below the maximum allowable. The stresses and safety factors in the humeri during flapping flight other than hovering will be between the values reported in Table 5 for gliding and hovering flight. Table 6 gives the mean values and standard deviations for the stresses and safety factors in the humeri for the birds and bats examined here. In general, the safety factors are about three times greater in gliding flight than on the downstroke in hovering. In every case, except for safety factors against failure due to shearing stresses in gliding flight, the mean safety factor in birds is greater than that for bats.

The result that wing bone stresses are in no way scale-dependent is at odds with the predictions of geometric similarity, which says that the stresses should increase directly with wing span (see above). This is due to a combination of the scaling patterns of both the relevant morphological variables and the imposed moments. While none of the

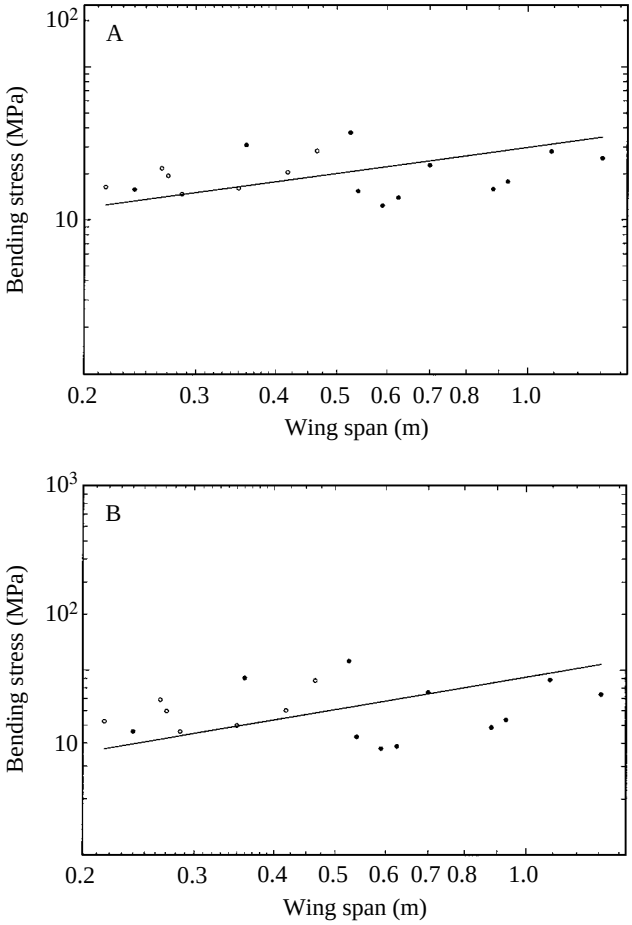

Fig. 5. (A) Bending stresses as a function of wing span in gliding flight. The correlation coefficient (0.197) is not significantly different from zero, indicating that there is no scale-dependence on bending stresses in gliding flight. (B) Bending stress as a function of wing span in hovering flight. The correlation coefficient (0.161) is also not significantly different from zero, indicating that there is no scale-dependence on bending stress in hovering flight. Filled circles, birds; open circles, bats.

morphological variables scaled differently from isometry, they did not scale exactly isometrically. Most of the imposed bending moments on the humeri did scale statistically differently from the predictions of geometric similarity (Table 4), and those that were not statistically different had wide fiducial limits about the slope. The combination of these results leads to the end result that, although there is some variation in wing bone stresses, these stresses are not scale-dependent.

The stresses in the long bones of land animals running at similar gaits have been calculated by Alexander (1977), Alexander and Vernon (1975), Alexander *et al.* (1979) and Rubin and Lanyon (1982). Their findings all agree that the stresses in the long bones do not vary in any systematic way with body size. This is the same result reported here for

Table 5. *Bending and shearing stresses in the humerus during gliding flight and on the downstroke in hovering*

Species	Body mass (kg)	Wing span (m)	Stress (MPa)	Safety factor
Birds				
Falco sparverius	0.072	0.59		
σ_g			12.4	10.8
σ_h			37.4	3.34
τ_g			0.86	109.0
τ_h			3.56	26.3
Puffinus lherminieri	0.082	0.625		
σ_g			14.0	8.93
σ_h			38.4	3.26
τ_g			4.49	20.8
τ_h			8.89	10.4
Mimus polyglottos	0.041	0.36		
σ_g			30.9	4.05
σ_h			90.5	1.38
τ_g			2.16	43.4
τ_h			9.46	9.90
Rallus longirostrus	0.22	0.525		
σ_g			37.3	3.35
σ_h			111.9	1.12
τ_g			7.61	12.3
τ_h			27.2	3.45
Buteo platypterus	0.295	0.93		
σ_g			17.8	7.02
σ_h			53.5	2.34
τ_g			5.59	16.8
τ_h			21.5	4.36
Bubulcus ibis	0.250	0.882		
σ_g			15.9	7.86
σ_h			48.6	2.57
τ_g			1.16	80.8
τ_h			5.76	16.3
Phalacrocorax auritus	1.50	1.31		
σ_g			25.3	4.94
σ_h			73.5	1.70
τ_g			4.51	20.8
τ_h			16.5	5.68
Seiurus aurocapillus	0.02	0.24		
σ_g			15.8	7.91
σ_h			46.3	2.70
τ_g			1.35	69.4
τ_h			6.55	14.3
Larus atricilla	0.305	1.09		
σ_g			28.1	4.45
σ_h			88.5	1.41
τ_g			3.57	35.0
τ_h			5.85	21.4
Catoptrophorus semipalmatus	0.21	0.70		
σ_g			22.8	5.48
σ_h			75.5	1.66
τ_g			1.09	86.0
τ_h			5.45	17.2

Table 5. *Continued*

Species	Body mass (kg)	Wing span (m)	Stress (MPa)	Safety factor
Otus asio	0.094	0.54		
σ_g			15.4	8.12
σ_h			43.3	2.89
τ_g			1.67	56.1
τ_h			6.36	14.7
Bats				
Artibeus phaeotis	0.011	0.285		
σ_g			14.7	5.10
σ_h			46.3	1.62
τ_g			0.80	70.3
τ_h			4.40	12.8
Phyllostomus discolor	0.039	0.465		
σ_g			28.3	2.65
σ_h			87.7	0.855
τ_g			1.54	36.5
τ_h			8.24	6.83
Tonatia sp.	0.012	0.265		
σ_g			21.8	3.44
σ_h			68.9	1.93
τ_g			1.62	34.7
τ_h			8.68	6.48
Rhogeessa tumida	0.004	0.216		
σ_g			16.4	4.57
σ_h			52.6	1.43
τ_g			0.29	194.0
τ_h			2.92	19.3
Glossophaga soricina	0.01	0.271		
σ_g			19.4	3.87
σ_h			59.6	1.26
τ_g			1.78	31.6
τ_h			7.89	7.13
Artibeus jamaicensis	0.037	0.418		
σ_g			20.5	3.66
σ_h			60.3	1.24
τ_g			4.69	12.0
τ_h			17.3	3.25
Carillia perspicillata	0.0195	0.35		
σ_g			16.1	4.65
σ_h			49.8	1.51
τ_g			3.98	14.1
τ_h			14.9	3.78

σ_g, bending stress in gliding; σ_h, bending stress in hovering; τ_g, shear stress in gliding; τ_h, shear stress in hovering, all in MPa.

Safety factor is the ratio between the breaking stress of wing bone material and the estimated stress.

Ultimate tensile stress of bird wing bone was taken to be 125 MPa and that of bat wing bone 75 MPa.

Ultimate shear strength was taken to be 75 % of the ultimate tensile strength.

Table 6. *Mean stresses (MPa) and safety factors, with standard deviations in parentheses, for the birds (*N*=11) and bats (*N*=7) used in this study*

	Birds		Bats	
	Stress	Safety factor	Stress	Safety factor
σ_g	21.4 (8.07)	6.63 (2.34)	19.6 (4.61)	3.99 (0.839)
σ_h	64.3 (25.04)	2.22 (0.795)	60.7 (14.1)	1.41 (0.338)
τ_g	3.30 (2.37)	50.0 (32.6)	2.10 (1.63)	56.2 (63.7)
τ_h	10.5 (7.85)	13.1 (7.19)	9.19 (5.22)	8.51 (5.68)

Symbols are defined in Table 5.

flying animals, except that the bending stresses in the wing bones of flying animals tend to be lower than those in the limb bones involved in terrestrial locomotion. This can adequately be explained by the result that bird and bat wing bone is not as strong as the compact bone of the limbs of terrestrial animals and, therefore, in order to ensure adequate safety factors, the imposed stresses must be kept at a lower level. The safety factors found here for bird and bat humeri in bending are quite similar to those reported elsewhere in the literature for running animals using force platforms and cine film (Alexander, 1981) and using strain gauges (Rubin and Lanyon, 1982).

Swartz *et al.* (1992) reported on the stresses in the wing bones of free-flying grey headed flying foxes (*Pteropus poliocephalus*). Their conclusion that shearing stress is significant in the wing bones of flying foxes is consistent with the results of the present mechanical model. Their reported longitudinal and shearing stresses in the humerus in mid-downstroke fall approximately between the values estimated here for gliding flight and hovering flight. However, their estimates of longitudinal stresses in the humerus during flapping flight are very close to the bending stresses that are estimated here to be present in gliding flight, while their shear stress estimates are similar to those estimated here for hovering flight. This indicates that the mechanical model presented here may slightly overestimate bending stresses, while underestimating shearing stresses. This does not, however, affect the result that the stresses in the humeri are not scale-dependent.

In conclusion, as a broken wing may be fatal to a flying animal, it should be expected that the safety factors in the wing bones should be at least as high as those found in other animals. From the results of this study, it appears that they are. The primary results, that the stresses in the wing bones do not vary in any systematic way with body size and that the bending stresses in the humeri of flying animals are lower than those in the limb bones of terrestrial animals while the safety factors are approximately the same, support Hill's (1950) working hypothesis that it is the mechanical properties of the structural materials that set the limits on the performance and design of organisms.

Appendix

Allometric equations (95 % fiducial limits; *r*) for the morphological variables measured in this study. The equations indicate how the variables relate to wingspan, *b*.

Body mass m_b

Birds $b = 1.30 m_b^{0.41}$ (0.443, 0.375; $r = 0.987$). (A1a)

Bats $b = 0.964 m_b^{0.31}$ (0.355, 0.277; $r = 0.964$). (A1b)

Wing area S

Birds $S = 0.134 b^{1.78}$ (1.89, 1.67; $r = 0.989$). (A2a)

Bats $S = 0.124 b^{1.83}$ (2.21, 1.51; $r = 0.943$). (A2b)

Second moment of area about the shoulder joint Q_2

Birds $Q_2 = 2.92 \times 10^{-3} b^{3.87}$ (3.65, 4.10; $r = 0.997$). (A3a)

Bats $Q_2 = 1.95 \times 10^{-3} b^{3.66}$ (3.99, 4.17; $r = 0.995$). (A3b)

Wing moment of inertia about the shoulder joint I_w

Birds $I_w = 9.23 \times 10^{-4} b^{5.08}$ (5.38, 4.80; $r = 0.984$) (A4a)
(from Kirkpatrick, 1990).

Neotropical bats
$I_w = 1.02 \times 10^{-3} b^{5.11}$ (5.57, 4.69; $r = 0.994$). (A4b)

Old World and neotropical bats combined
$I_w = 8.52 \times 10^{-4} b^{4.96}$ (5.22, 4.72; $r = 0.982$) (A4c)
(data for Old World bats from Tholleson and Norberg, 1991).

Insects $I_w = 3.06 \times 10^{-4} b^{4.74}$ (5.16, 4.35; $r = 0.989$). (A4d)

Second moment of area of bone cross-sections

Bird humerus
$I_h = 6.02 \times 10^{-11} b^{4.19}$ (4.45, 3.94; $r = 0.984$). (A5a)

Bat humerus
$I_h = 2.68 \times 10^{-11} b^{4.42}$ (4.97, 3.92; $r = 0.964$). (A5b)

Bird proximal radio-ulna
$I_{pru} = 3.7 \times 10^{-11} b^{4.22}$ (4.55, 3.51; $r = 0.977$). (A5c)

Bat proximal radius
$I_{pr} = 1.24 \times 10^{-11} b^{3.87}$ (4.80, 3.13; $r = 0.875$). (A5d)

Bird distal radio-ulna
$I_{dru} = 2.29 \times 10^{-11} b^{3.46}$ (4.38, 2.74; $r = 0.942$). (A5e)

Bat distal radius
$I_{dr} = 1.71 \times 10^{-11} b^{4.53}$ (6.66, 3.08; $r = 0.897$). (A5f)

Bird metacarpus
$I_m = 1.28 \times 10^{-11} b^{3.62}$ (4.86, 2.69; $r = 0.918$). (A5g)

Bat metacarpus
$I_m = 5.01 \times 10^{-13} b^{3.17}$ (5.80, 1.73; $r = 0.829$). (A5h)

Polar moment of area of bone cross sections

Bird humerus
$J_h = 1.18 \times 10^{-10} b^{4.23}$ (4.52, 3.95; $r = 0.979$). (A6a)

Bat humerus
$J_h = 5.19 \times 10^{-11} b^{4.38}$ (4.94, 3.88; $r = 0.963$). (A6b)

Bird proximal radio-ulna
$J_{pru} = 8.17 \times 10^{-11} b^{3.88}$ (4.14, 3.63; $r = 0.983$). (A6c)

Bat proximal radius
$J_{pr} = 2.19 \times 10^{-11} b^{3.79}$ (4.45, 3.23; $r = 0.933$). (A6d)

Bird distal radio-ulna

$$J_{\mathrm{dru}} = 5.23 \times 10^{-11} b^{3.63}\ (4.64, 2.84;\ r = 0.937)\,. \tag{A6e}$$

Bat distal radius

$$J_{\mathrm{dr}} = 3.60 \times 10^{-11} b^{4.36}\ (6.13, 3.11;\ r = 0.922)\,. \tag{A6f}$$

Bird metacarpus

$$J_{\mathrm{m}} = 3.77 \times 10^{-11} b^{3.86}\ (5.78, 2.58;\ r{=}0.835)\,. \tag{A6g}$$

Bat metacarpus

$$J_{\mathrm{m}} = 2.21 \times 10^{-12} b^{3.43}\ (8.39, 1.40;\ r = 0.466)\,. \tag{A6h}$$

I would like to thank Colin J. Pennycuick for his assistance throughout the course of this study. Jay Savage, Eugene Eckstein, Leo Sternberg, Kathleen Sullivan, Doyle McKey, Catherine Sahley and Joseph Slowinski all helped in various ways. Laura Quinn of the Florida Keys Wildbird Rehabilitation Center provided many of the bird specimens. A Tropical Biology Fellowship from the University of Miami and the Sea and Sky foundation all provided some support for this project.

References

ABBOTT, I. H. AND VON DOENHOFF, A. E. (1959). *Theory of Wing Sections*. New York: Dover.

ALEXANDER, R. MCN. (1977). Allometry of the limbs of Antelopes (Bovidae). *J. Zool., Lond.* A **183**, 125–146.

ALEXANDER, R. MCN. (1981). Factors of safety in the structure of mammals. *Science Prog.* **67**, 109–130.

ALEXANDER, R. MCN., MALOIY, G. M. O., HUNTER, B. AND NTURIBI, J. (1979). Mechanical stresses in fast locomotion of buffalo (*Syncerus caffer*) and elephant (*Loxodonta africana*). *J. Zool., Lond.* A **189**, 135–144.

ALEXANDER, R. MCN. AND VERNON, A. (1975). The mechanics of hopping by kangaroos (Macropodidae). *J. Zool., Lond.* A **177**, 265–303.

CURREY, J. D. (1987). The evolution of the mechanical properties of amniote bone. *J. Biomech.* **20**, 1035–1044.

CURREY, J. D. (1988). The effect of porosity and mineral content on the Young's modulus of elasticity of compact bone. *J. Biomech.* **21**, 131–139.

ELLINGTON, C. P. (1984). The aerodynamics of hovering insect flight. II. Morphological parameters. *Phil. Trans. R. Soc. Lond. B* **305**, 17–40.

GREENWALT, C. H. (1962). Dimensional relationships for flying animals. *Smithson. misc. collns.* **144**(2) 1–46.

GREENWALT, C. H. (1975). The flight of birds: the significant dimensions, their departure from the requirements for dimensional similarity and the effect on flight aerodynamics of that departure. *Trans Am. phil. Soc.* **64**(4) 1–67.

HILL, A. V. (1950). The dimensions of animals and their muscular dynamics. *Science Prog.* **38**, 209–230.

HOFMAN, M. A. (1988). Allometric scaling in palaeontology: a critical survey. *Human Evol.* **3**, 177–188.

KIRKPATRICK, S. J. (1990). The moment of inertia of bird wings. *J. exp. Biol.* **151**, 489–494.

NORBERG, U. M. (1990). *Vertebrate Flight*. Berlin: Springer-Verlag.

PENNYCUICK, C. J. (1967). The strength of the pigeon's wing bones in relation to their function. *J. exp. Biol.* **46**, 219–133.

PENNYCUICK, C. J. (1989). *Bird Flight Performance: A Practical Calculation Manual*. Oxford: Oxford University Press.

PENNYCUICK, C. J. (1990). Predicting wingbeat frequency and wavelength of birds. *J. exp. Biol.* **150**, 171–185.

RAYNER, J. M. V. (1985). Linear relations in biomechanics: the statistics of scaling functions. *J. Zool., Lond.* A **206**, 415–439.

RUBIN, C. T. AND LANYON, L. E. (1982). Limb mechanics as a function of speed and gait: a study of functional strains in the radius and tibia of horse and dog. *J. exp. Biol*. **101**, 187–211.

SOTAVALTA, O. (1954). The effect of wing inertia on the wing-stroke frequency of moths, dragonflies and cockroach. *Annls ent. Fenn*. **20**, 93–101.

SWARTZ, S. M., BENNETT, M. B. AND CARRIER, D. R. (1992). Wing bone stresses in free flying bats and the evolution of skeletal design for flight. *Nature* **359**, 726–729.

THOLLESSON, M. AND NORBERG, U. M. (1991). Moments of inertia of bat wings and body. *J. exp. Biol*. **158**, 19–35.

WAINWRIGHT, S. A., BIGGS, W. D., CURREY, J. D. AND GOSLINE, J. M. (1976). *Mechanical Design in Organisms*. Princeton, New Jersey: Princeton University Press.

WEIS-FOGH, T. (1973). Quick estimates of flight fitness in hovering animals, including a novel mechanism for lift production. *J. exp. Biol*. **59**, 169–230.

YAMADA, H. (1970). *Strength of Biological Materials*. Baltimore, MD: Williams and Wilkens.